AMERICAN SOCIETY FOR MICROBIOLOGY | Molecular and Cellular Biology®

RESEARCH ARTICLE

hnRNP K Supports High-Amplitude D Site-Binding Protein mRNA (*Dbp* mRNA) Oscillation To Sustain Circadian Rhythms

Paul Kwangho Kwon,[a] Kyung-Ha Lee,[a]* Ji-hyung Kim,[b] Sookil Tae,[c] Seokjin Ham,[a]* Young-Hun Jeong,[a] Sung Wook Kim,[c] Byunghee Kang,[c] Hyo-Min Kim,[c] Jung-Hyun Choi,[a]* Hee Yi,[d] Hyun-Ok Ku,[d] Tae-Young Roh,[a,c] Chunghun Lim,[b] Kyong-Tai Kim[a,c]

[a]Department of Life Sciences, Pohang University of Science and Technology, Pohang, Gyeongbuk, Republic of Korea
[b]School of Life Sciences, Ulsan National Institute of Science and Technology, Ulsan, Republic of Korea
[c]Division of Integrative Biosciences and Biotechnology, Pohang University of Science and Technology, Pohang, Gyeongbuk, Republic of Korea
[d]Vet Drugs and Biologics Division, Animal and Plant Quarantine Agency, Gimcheon, Gyeongsangbuk, Republic of Korea

ABSTRACT Circadian gene expression is defined by the gene-specific phase and amplitude of daily oscillations in mRNA and protein levels. D site-binding protein mRNA (*Dbp* mRNA) shows high-amplitude oscillation; however, the underlying mechanism remains elusive. Here, we demonstrate that heterogeneous nuclear ribonucleoprotein K (hnRNP K) is a key regulator that activates *Dbp* transcription via the poly(C) motif within its proximal promoter. Biochemical analyses identified hnRNP K as a specific protein that directly associates with the poly(C) motif *in vitro*. Interestingly, we further confirmed the rhythmic binding of endogenous hnRNP K within the *Dbp* promoter through chromatin immunoprecipitation as well as the cycling expression of hnRNP K. Finally, knockdown of hnRNP K decreased mRNA oscillation in both *Dbp* and *Dbp*-dependent clock genes. Taken together, our results show rhythmic protein expression of hnRNP K and provide new insights into its function as a transcriptional amplifier of *Dbp*.

KEYWORDS circadian rhythm, Dbp, hnRNP K, mRNA oscillation

Circadian rhythm is present in living organisms and reflects the elaborate nature of biological systems. Most living organisms have a circadian rhythm, which helps to synchronize daily changes in gene expression, metabolism, and physiology (1). The circadian clock system is modulated by transcriptional, posttranscriptional, translational, and posttranslational regulation (2–4). Recently, posttranscriptional regulation of clock genes by RNA-binding proteins such as hnRNP Q (5–8), PTB (9), hnRNP D (10), hnRNP A1 (11), hnRNP R (12), and hnRNP K (13) was shown to play a role in circadian rhythm.

As a strong poly(C)-binding protein (14–17), heterogeneous nuclear ribonucleoprotein K (hnRNP K) has been revealed to be involved in multiple gene expression processes when bound to single-stranded DNA or RNA, including the regulation of chromatin modification, transcription, posttranscriptional regulation (18, 19), and translation (17). Among these multiple mechanisms of gene expression regulation, hnRNP K modulates transcription by interacting with TATA-binding protein (TBP) (20, 21) and by stabilizing DNA secondary structures as a transactivator (22–24). Specifically, it was reported that hnRNP K could bind directly to C-rich single-stranded DNA within the tyrosine hydroxylase (Th), eukaryotic translation initiation factor 4E (eIF4E), c-myc, steroid receptor coactivator 1 (SRC 1A), and human vascular endothelial growth factor (VEGF) gene promoters to activate transcription (24–28). It was also reported that large intergenic noncoding RNAs (lincRNAs) could physically associate with hnRNP K to induce proper genomic localization, which results in the repression of p53-dependent transcriptional responses (29). Here, we discovered that hnRNP K fostered D site-binding protein mRNA (*Dbp* mRNA) transcription through the poly(C) motif and played

Citation Kwon PK, Lee K-H, Kim J-H, Tae S, Ham S, Jeong Y-H, Kim SW, Kang B, Kim H-M, Choi J-H, Yi H, Ku H-O, Roh T-Y, Lim C, Kim K-T. 2020. hnRNP K supports high-amplitude D site-binding protein mRNA (*Dbp* mRNA) oscillation to sustain circadian rhythms. Mol Cell Biol 40:e00537-19. https://doi.org/10.1128/MCB.00537-19.

Address correspondence to Kyong-Tai Kim, ktk@postech.ac.kr.

* Present address: Kyung-Ha Lee, Division of Bio-technology and Convergence, Daegu Haany University, Gyeongsan, Gyeongbuk, Republic of Korea; Seokjin Ham, Department of Biological Sciences, Korea Advanced Institute of Science and Technology, Daejeon, Republic of Korea; Jung-Hyun Choi, Department of Biochemistry and Goodman Cancer Research Centre, McGill University, Montreal, Quebec, Canada.

Received 1 November 2019
Returned for modification 13 December 2019
Accepted 20 December 2019
Accepted manuscript posted online 6 January 2020
Published 27 February 2020

a role in circadian rhythm. *Dbp* mRNA oscillation is known for having high amplitude among clock genes (30, 31). Also, a mood disorder, bipolar disorder, was reported to be associated with decreased levels of both *Dbp* mRNA oscillation amplitude and expression (32). *Dbp* protein can bind to the D-box elements like with many other D-box *trans*-acting regulators, such as thyrotroph embryonic factor (Tef), hepatic leukemia factor (Hlf), and nuclear factor interleukin 3 regulated (Nfil3). Dbp, Tef, and Hlf act as transcription activators, while Nfil3 acts as a transcription repressor (33). Also, Dbp regulates other core clock genes, such as Period genes, Rev-erb genes, and ROR genes (33–37). It was reported that *Dbp* mRNA oscillation is maintained by the BMAL1-CLOCK complex via multiple E boxes (4, 38–40). Recently, the poly(C) motif within the *Dbp* promoter was reported as a novel *cis*-acting element that regulates *Dbp* mRNA oscillation (41). However, little is known about the *trans*-acting factor that supports high-amplitude *Dbp* mRNA oscillation through the interaction with the poly(C) motif.

In this study, we investigated the *trans*-acting factor of the poly(C) motif that could induce a higher amplitude of *Dbp* mRNA oscillation. Thus, in addition to the previous function of hnRNP K as a stabilizer of *Per3* mRNA, we proposed a new function of hnRNP K as a transcriptional activator of circadian rhythm.

RESULTS

hnRNP K controls the expression of *Dbp* mRNA and not its stability. To screen *trans*-acting factors that regulate the expression of *Dbp* mRNA, we knocked down several RNA-binding proteins, such as hnRNP Q (5–8), PTB (9), hnRNP D (10), hnRNP A1 (11), hnRNP R (12), and hnRNP K (13). Interestingly, we found that hnRNP K was the only factor that could regulate the *Dbp* mRNA level significantly (see Fig. S1 in the supplemental material). Next, we confirmed the knockdown efficiency of the hnRNP K small interfering RNA (siRNA) pool by immunoblotting (IB) (Fig. 1A). Cells transfected with the hnRNP K siRNA pool showed an approximately 70% decrease in hnRNP K protein levels compared to the siRNA-transfected control group. Furthermore, we checked cell viability using the 3-(4,5-dimethyl-2-thiazolyl)-2,5-diphenyl-2H-tetrazolium bromide (MTT) assay. Under our experimental conditions, the knockdown of hnRNP K did not significantly affect cell viability (Fig. 1B). We also compared the endogenous levels of *Dbp* pre-mRNA and mature mRNA. The levels of both of these types of *Dbp* mRNA decreased after knockdown of hnRNP K (Fig. 1C). Per3, which has been reported to retain mRNA stability through hnRNP K, was used as a positive control (13), while Cry1 was used as a negative control. The result suggested that transcriptional activation of *Dbp* might be decreased by knockdown of hnRNP K. Next, we examined the effects of hnRNP K on other D-box *trans*-acting regulators, i.e., Tef, Hlf, and Nfil3, by measuring mRNA levels during knockdown of hnRNP K. We confirmed that the *Dbp* mRNA level decreased significantly during knockdown of hnRNP K, while the *Tef* and *Hlf* mRNA levels showed a nonsignificant decrease (Fig. 1D). This indicates that the primary target of hnRNP K is the D-box regulator Dbp, not other D-box regulators. In addition, we elucidated the kinetics of mRNA decay to confirm the possibility of mRNA degradation, which was previously reported to be related to the function of hnRNP K (13). To examine the role of hnRNP K in *Dbp* mRNA expression regulation, the mRNA stabilities of the control group and the siRNA knockdown group were compared under treatment with actinomycin D, which inhibits transcription. The data showed that the half-life of *Dbp* mRNA did not change during the knockdown of hnRNP K, while the half-life of *Per3* mRNA showed a decrease, as has been previously reported (Fig. 1E). Also, we confirmed that *Tbp* mRNA stability, which was used as a control, was barely affected by the knockdown of hnRNP K (see Fig. S2 in the supplemental material). These results indicate that hnRNP K may regulate Dbp not by mRNA degradation but by transcriptional activation.

The activities of specific promoter regions of *Dbp* are affected by hnRNP K. We compared the promoter activity of wild-type short [WT(Short)] (promoter region containing 564 bp from the transcription start site [TSS]) and wild-type long [WT(Long)] (promoter region containing 1,500 bp from the TSS) promoter forms during the knockdown of hnRNP K, using the constructs from a previously reported study (41). We

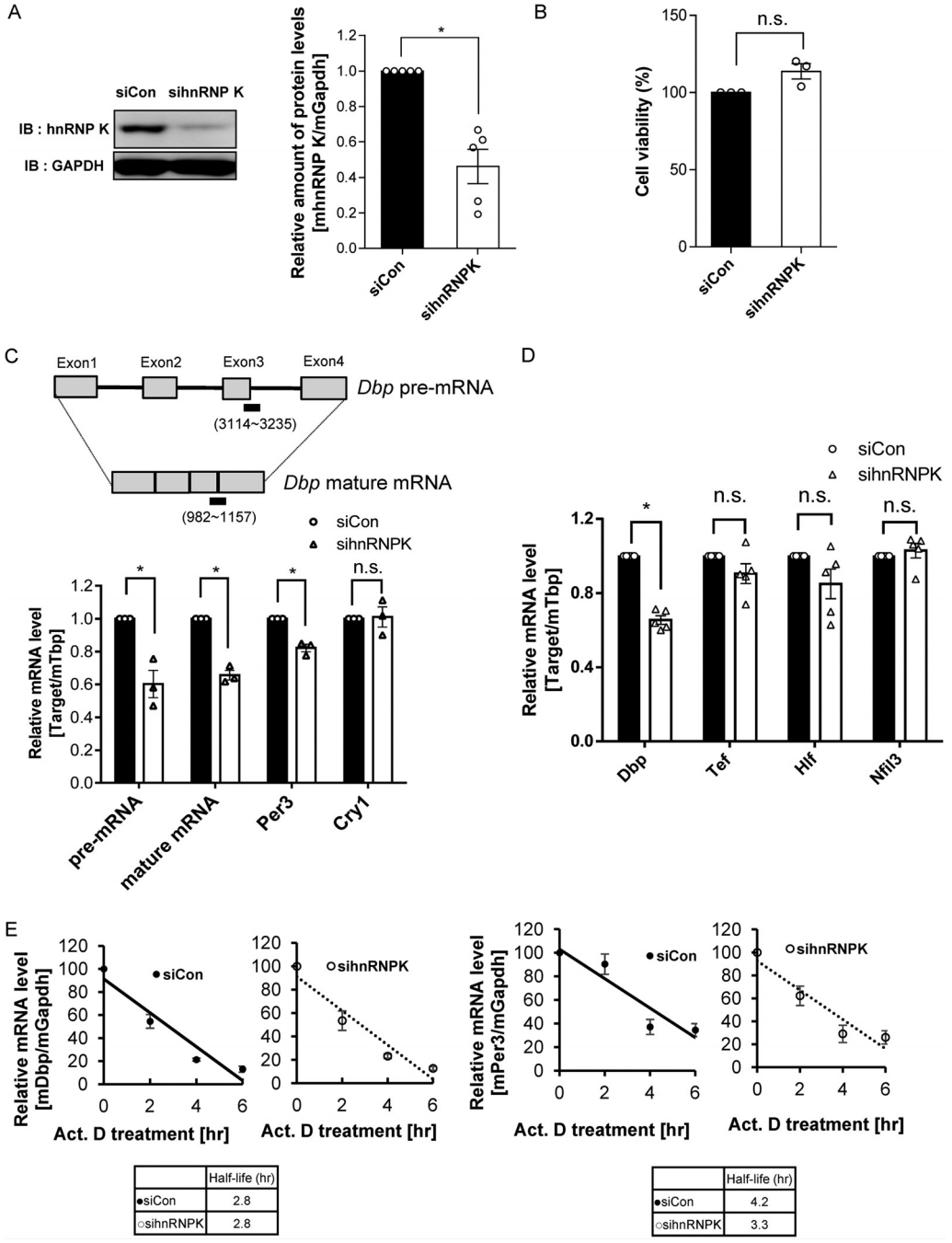

	Half-life (hr)
●siCon	2.8
○sihnRNPK	2.8

	Half-life (hr)
●siCon	4.2
○sihnRNPK	3.3

FIG 1 hnRNP K controls the *Dbp* mRNA expression but not stability. (A) Knockdown of hnRNP K was mediated by siRNA transfection in NIH 3T3 cells. The group with hnRNP K siRNA pool transfection showed a significant decrease of the hnRNP K protein level ($n = 5$; *, $P < 0.05$ by the unpaired *t* test). (B) MTT assay showed that the knockdown of hnRNP K did not significantly affect the viability of the NIH 3T3 cells ($n = 3$; n.s., not significant; $P < 0.05$ [by the unpaired *t* test]). (C) *Dbp* pre-mRNA and mature mRNA levels were measured during the knockdown of hnRNP K. Both levels were decreased. *Per3* was used as a positive control, and *Cry1* was used as a negative control. The locations of primers are shown ($n = 3$; n.s., not significant; *, $P < 0.05$ by two-way ANOVA followed by Sidak's multiple-comparison test). (D) The mRNA levels of other D-box *trans*-acting regulators were measured after transfection of siRNAs. The data showed that the *Dbp* mRNA level was significantly lowered, while those for other D-box regulators (*Tef*, *Hlf*, and *Nfil3*) were not ($n = 5$; n.s., not significant; *, $P < 0.05$ by two-way ANOVA followed by Sidak's multiple-comparison test). (E) During knockdown of hnRNP K, *Dbp* mRNA decay rates were not altered by treatment with the transcription inhibitor actinomycin D. *Per3* was used as a positive control, and its decay rate was decreased. (siCon group, $y = -14.71x + 91.323$; sihnRNP K group, $y = -14.603x + 91.192$) ($n = 3$). Error bars indicate SEM.

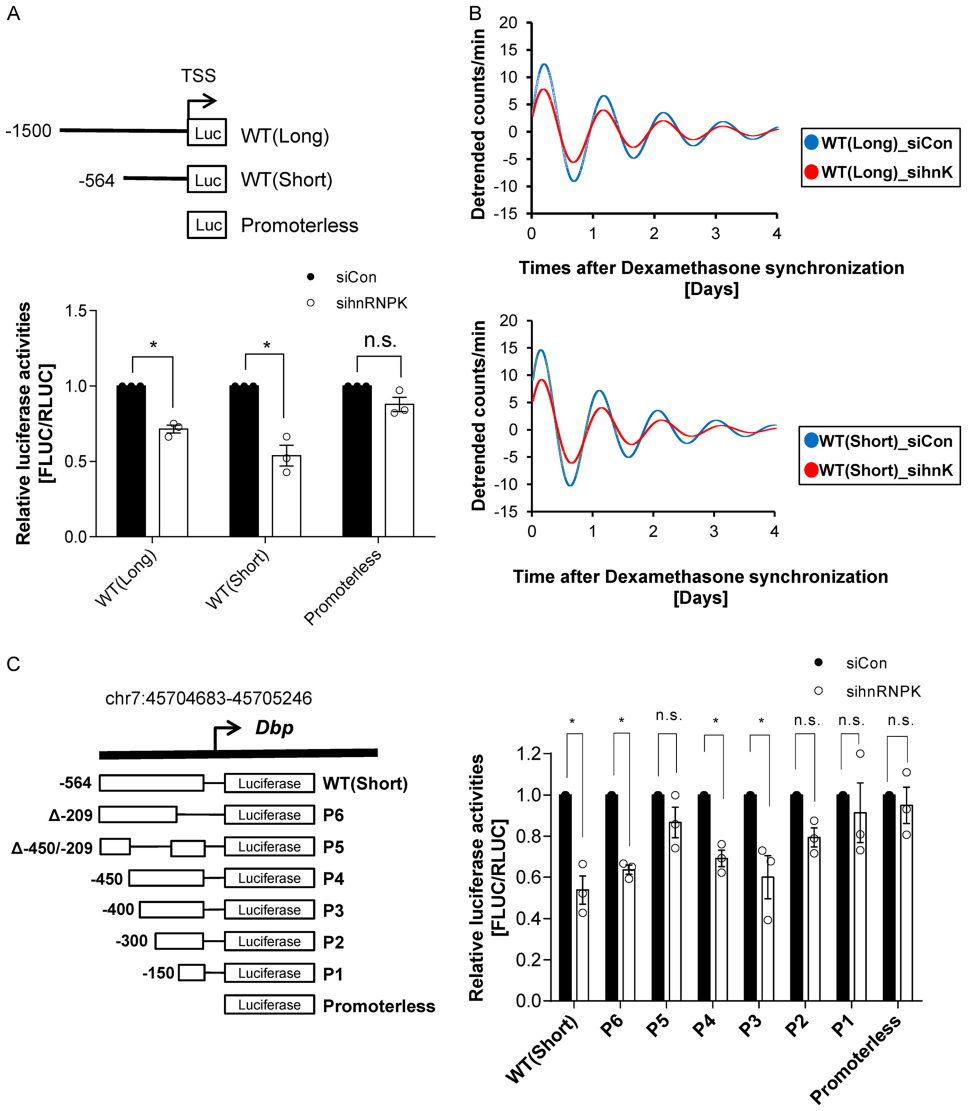

FIG 2 The activity of specific promoter regions of *Dbp* is affected by hnRNP K. (A) Along with WT(Short) promoter activity (the region contained 564 bp from the TSS), the level of WT(Long) promoter activity (the region contained 1,500 bp from the TSS) was similarly downregulated by the lack of hnRNP K, while that of a promoterless vector was not ($n = 3$; n.s., not significant; *, $P < 0.05$ by two-way ANOVA followed by Sidak's multiple-comparison test). (B) Representative detrended bioluminescence recordings of WT(Short):LUC and WT(Long):LUC were measured with luciferase reporter-transfected NIH 3T3 cells after dexamethasone synchronization during knockdown of hnRNP K, which showed a decrease in the amplitude levels of WT(Short):LUC and WT(Long):LUC. sihnK, sihnRNP K. (C) Knockdown of hnRNP K decreased the levels of P3, P4, P6, and WT(Short) promoter activity ($n = 3$; n.s., not significant; *, $P < 0.05$ by two-way ANOVA followed by Sidak's multiple-comparison test). Error bars indicate SEM.

confirmed that the levels of WT(Short) and WT(Long) promoter expression were downregulated by knockdown of hnRNP K (Fig. 2A). These results suggested that the 564-bp promoter region of *Dbp* was the critical region for the regulation by hnRNP K. Also, we found that the oscillation amplitude levels of the WT(Short) and WT(Long) promoters were decreased in a real-time luminescence experiment when hnRNP K was knocked down, while their periods were not significantly changed (Fig. 2B). Next, we quantified the promoter activity of constructs that contained serially deleted proximal promoter regions (Fig. 2C). The data showed that the promoter activities of the P3, P4, P6, and WT(Short) constructs, which were used as previously shown (41), decreased significantly when hnRNP K was downregulated. Thus, we hypothesized that hnRNP K could control *Dbp* expression through its interaction with the regions between positions −300 and −400 from the TSS of *Dbp*.

hnRNP K binds to the single-stranded poly(C) motif directly. Although the CCT element has already been reported to be a binding target of hnRNP K, functional confirmation of this interaction and prediction of the function of hnRNP K on this motif have not previously been investigated (17, 20, 22, 23). For this reason, we searched a database that contains 1,056 hnRNP K-bound promoter genes from hnRNP K chromatin immunoprecipitation sequencing (ChIP-Seq) (29) (Fig. 3A). To identify specific motifs that are predicted to function in transcription by GOMo, we utilized MEME-ChIP to analyze the data from hnRNP K ChIP-Seq (42, 43, 48). Through this, we detected the CCC motif and the CCT motif within the proximal promoter regions of hnRNP K-bound promoter genes (Fig. 3B). Both the CCC motif and the CCT motif were also predicted to function in transcription (Fig. S3).

Interestingly, it was reported that a pair of poly(C) motifs within the *Dbp* promoter supported *Dbp* mRNA oscillation (41). Thus, we analyzed the genes which contained a pair of poly(C) motifs. In the search for the poly(C) motif-binding factor, we pulled down proteins that were bound onto poly(C) oligonucleotides. Descriptions of the forward and reverse poly(C) motif sequences are provided in Fig. 3C. We attached biotin to the 5′nucleotide (Solgent, South Korea) of the forward sequence 5′CCGCCTCCAGCGCCTC CTCC3′ and the reverse complementary sequence 5′GGAGGAGGCGCTGGAGGCGG3′ and performed pulldown experiments with streptavidin in HEK293A cells. First, we found that almost no proteins were pulled down with the duplex form of the oligonucleotide (data not shown). Thus, we presumed that the single-strand oligonucleotide of the poly(C) motif might interact with certain unknown transcription factors. Surprisingly, we found that a single, thick protein band was detected when we used the forward poly(C) motif single-strand oligonucleotide, which was identified as hnRNP K by mass spectrometry (see Fig. S4A in the supplemental material). We also detected the binding of hnRNP K using anti-hnRNP K at the poly(C) motif (Fig. S4B).

To confirm the direct binding of hnRNP K to the poly(C) motif oligonucleotide, we purified glutathione *S*-transferase (GST) and GST-hnRNP K proteins and performed pulldown experiments with a 5′-biotinylated poly(C) motif and 5′-biotinylated poly(C) mutant (Fig. 3D). We confirmed through immunoblotting that GST-hnRNP K was detected only in the group pulled down with the wild-type oligonucleotide (Fig. 3D). This demonstrated that hnRNP K binds directly to the poly(C) motifs of *Dbp* promoter regions *in vitro*.

Thus, we hypothesized that hnRNP K might activate *Dbp* mRNA expression through the poly(C) motif within the *Dbp* promoter. To confirm this, we conducted a promoter assay with WT(Short) and the poly(C) mutant during knockdown of hnRNP K. While this clearly decreased the promoter activity of WT(Short), the promoter activity of the poly(C) mutant changed only a little (Fig. 3E). We also overexpressed hnRNP K using a human influenza virus hemagglutinin (HA) tag to assess promoter activity. Overexpression of hnRNP K increased WT(Short) promoter activity only (see Fig. S5 in the supplemental material).

Next, we compared the endogenous *Dbp* mRNA levels in WT cells and poly(C)-deleted cells during the knockdown of hnRNP K. We confirmed that hnRNP K affected *Dbp* mRNA expression in both cell types; however, the decrease of *Dbp* mRNA expression was significantly greater when the poly(C) motif was intact (see Fig. S6 in the supplemental material). Thus, we thought that hnRNP K could activate the endogenous *Dbp* mRNA expression through the poly(C) motif.

Next, we analyzed the KH3 domain sequence of hnRNP K (see Fig. S7A in the supplemental material), which is a single-stranded-DNA-binding domain (44–46). Using the Ensembl database, we found that the KH3 domains of several eutherian mammals aligned perfectly (Fig. S7B). This result suggests that hnRNP K binding to the promoter region of *Dbp* could be a critical regulatory mechanism for *Dbp* transcription in eutherian mammals.

hnRNP K binds to the endogenous *Dbp* promoter rhythmically. Previously, we confirmed that hnRNP K bound to the poly(C) motif *in vitro* and predicted that this

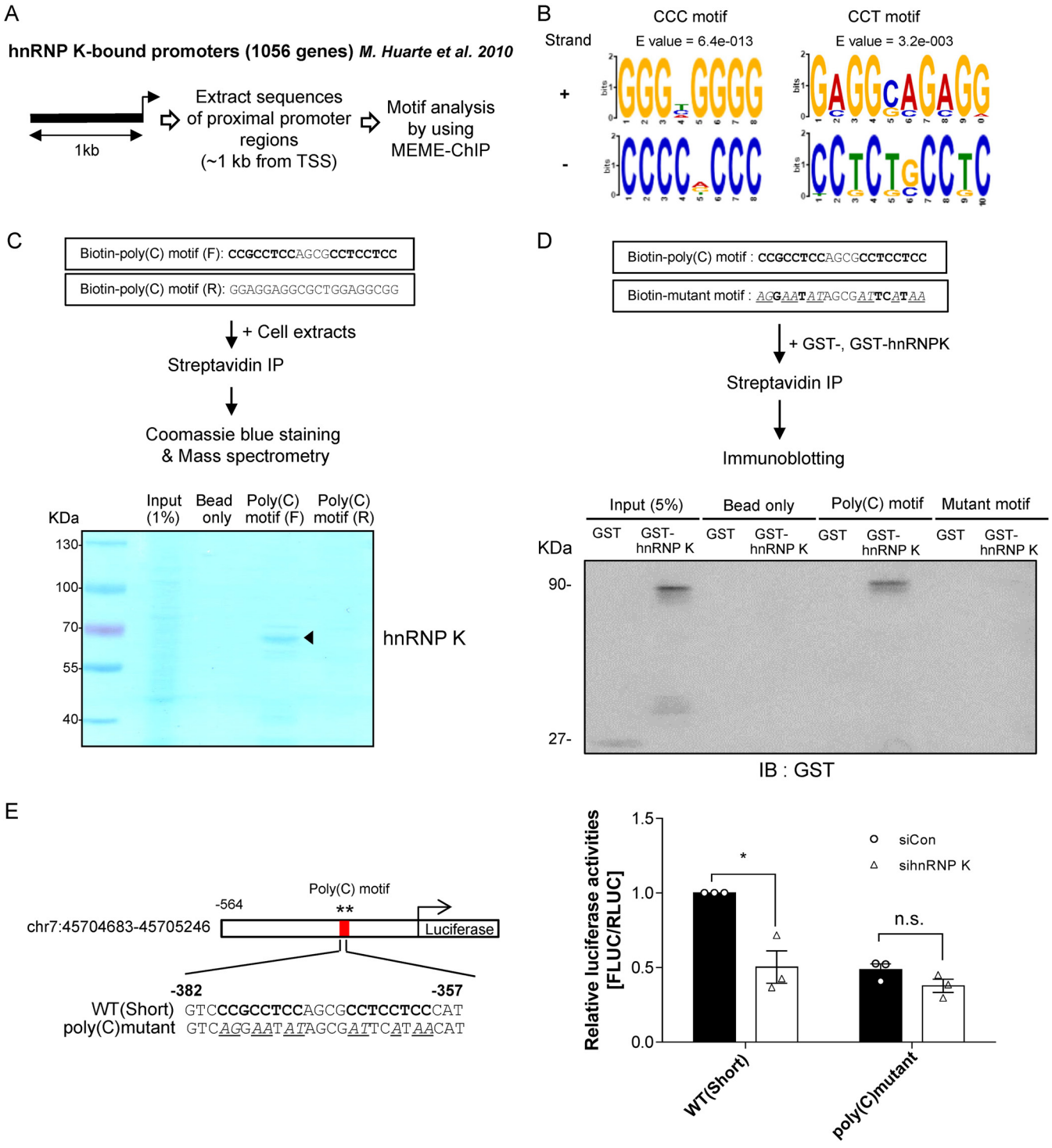

FIG 3 hnRNP K binds to the single-stranded poly(C) motif directly. (A) Schematic description of the motif analysis. Proximal promoter regions of 1,056 genes were analyzed using the database from reference 29. (B) Motif analysis showed that the CCC motif was frequently found along with a CCT motif. (C) Coomassie blue staining showed that one thick band was bound onto the forward poly(C) motif oligonucleotide, which was identified as hnRNP K by mass spectrometry. In contrast, there were no prominent proteins detected at the complementary poly(C) motif oligonucleotide. (D) Purification of GST and GST-hnRNP K was also carried out for pulldown assay. GST-hnRNP K was detected at the wild-type oligonucleotide but not at the mutant oligonucleotide, which demonstrates that hnRNP K is directly bound to the poly(C) motif. (E) To identify the effect of knockdown of hnRNP K on WT(Short) and the poly(C) mutant, a promoter assay was conducted with siRNA transfection. It showed a significant decrease only for WT(Short) promoter activity ($n = 3$; n.s., not significant; *, $P < 0.05$ by two-way ANOVA followed by Sidak's multiple-comparison test). Error bars indicate SEM.

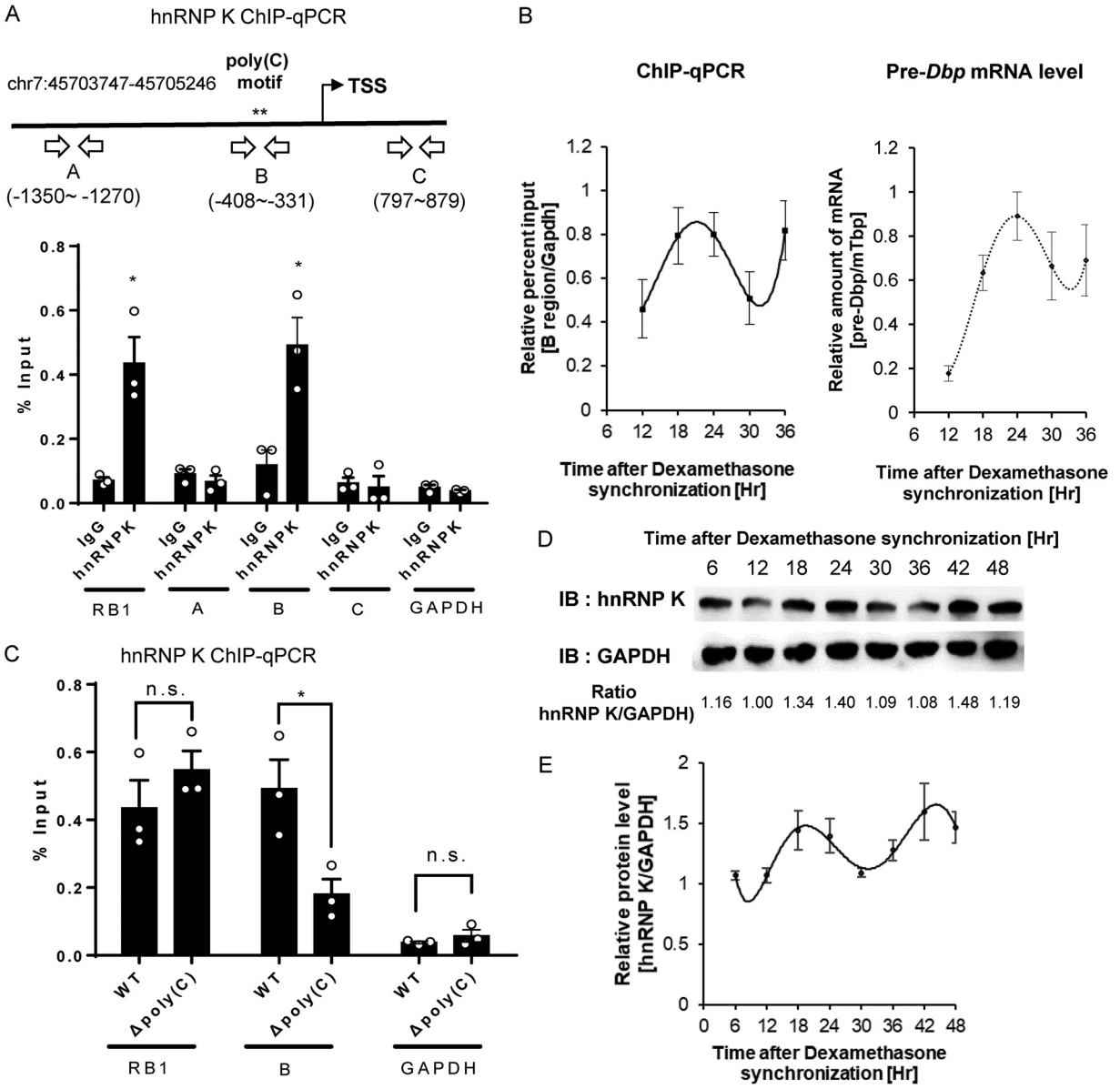

FIG 4 hnRNP K binds to the endogenous *Dbp* promoter rhythmically. (A) Endogenous binding of hnRNP K on proximal promoter regions of *Dbp* was confirmed by using ChIP assay. A, B, and C indicate genomic regions. RB1 was used as a positive control, while GAPDH was used as a negative control ($n = 3$; n.s., not significant; *, $P < 0.05$ by two-way ANOVA followed by Sidak's multiple-comparison test). (B) Rhythmic binding of hnRNP K was confirmed through triggering mRNA oscillation in NIH 3T3 cells. *Dbp* pre-mRNA levels showed a proportional relationship with the binding levels of hnRNP K. Relative percent input indicates the percent input level normalized by the GAPDH percent input level ($n = 3$). (C) hnRNP K ChIP data showed that the binding level of hnRNP K on the B region was decreased in poly(C)-deleted cells compared to the WT. However, RB1, which was used as a positive control, and GAPDH, which was used as a negative control, were not significantly affected ($n = 3$; *, $P < 0.05$ by two-way ANOVA followed by Sidak's multiple-comparison test). (D) After triggering the circadian rhythm by dexamethasone treatment, the levels of total hnRNP K protein were measured. GAPDH was used as a control. (E) Oscillatory expression levels of total hnRNP K protein were quantified ($n = 4$). Error bars indicate SEM.

would allow hnRNP K to function as a transcriptional activator by using Gene Ontology for Motifs (GOMo). We then examined the endogenous binding of hnRNP K to the proximal promoter region of *Dbp* using a chromatin immunoprecipitation (ChIP) assay, because previously reported ChIP-seq data did not show *Dbp* as a target gene of hnRNP K (29). The ChIP results showed that hnRNP K specifically bound to region 2 (B), which contains the poly(C) motif between positions −300 and −400 from the TSS. Region 1 (A) and region 3 (C) were not bound by hnRNP K (Fig. 4A). The RB1 gene, to which hnRNP K binds robustly, was used as a positive control, while the glyceraldehyde-3-

phosphate dehydrogenase (GAPDH) gene was used as a negative control (29). Next, we investigated whether the binding of hnRNP K was rhythmically influenced by dexamethasone synchronization, which induces mRNA circadian oscillation of clock genes, to further clarify the involvement of hnRNP K in *Dbp* transcription. We found that the oscillation of *Dbp* pre-mRNA levels correlated with the rhythmic binding of hnRNP K (Fig. 4B). Additionally, we compared hnRNP K ChIP data for WT cells to hnRNP K ChIP data for poly(C)-deleted cells, which showed that the binding level of hnRNP K on region 2 (B) was decreased in poly(C)-deleted cells. However, the binding levels of hnRNP K on RB1 and GAPDH were not significantly changed (Fig. 4C). Furthermore, we confirmed that the protein levels of hnRNP K showed oscillatory patterns after dexamethasone synchronization (Fig. 4D and E). Also, we confirmed the subcellular protein cycling levels of hnRNP K by subcellular fractionation of NIH 3T3 cells. These data suggest that the rhythmic cycling of nuclear hnRNP K proteins could be a major contributing factor to the rhythmic binding of hnRNP K (see Fig. S8A and B in the supplemental material).

hnRNP K supports high-amplitude *Dbp* mRNA oscillation and *Dbp*-dependent clock genes such as *Period2*, *Rev-erbα*, and *RORβ*. The circadian rhythm of *Dbp* mRNA in NIH 3T3 cells was also measured after triggering oscillation with dexamethasone to clarify the role of hnRNP K in maintaining high-amplitude *Dbp* mRNA oscillation. Quantification of circadian rhythm oscillation under hnRNP K knockdown revealed a decrease in the *Dbp* mRNA oscillation amplitude (Fig. 5A). Moreover, we investigated the mRNA oscillation levels of other *Dbp*-dependent clock genes, *Per2*, *Rev-erbα*, and *RORβ*, during the knockdown of hnRNP K (37, 41). Interestingly, we found that the mRNA oscillation amplitudes of *Per2*, *Rev-erbα*, and *RORβ* were lowered by the knockdown of hnRNP K after dexamethasone synchronization, while the mRNA oscillation amplitude of *Cry1* was not (Fig. 5A). eIF4e was used as a negative control (28). Next, we identified whether the direct effect of hnRNP K could regulate the *Dbp*-dependent clock genes by using the poly(C)-deleted cells. We knocked down hnRNP K and harvested at the peak (24 h) and trough (12 h) times after dexamethasone synchronization. We then compared the *Dbp*, *Per2*, *Rev-erbα*, *RORβ*, and *Cry1* mRNA expression levels at the peak time. The result showed that the fold level of *Cry1*, which was used as a negative control, was not changed, while the levels of *Dbp*, *Per2*, *Rev-erbα*, and *RORβ* were significantly decreased when hnRNP K was lowered. However, those changes were not seen when the poly(C) motif within the *Dbp* promoter was deleted (see Fig. S9 in the supplemental material). The poly(C)-deleted cells showed mRNA expression levels of *Dbp*-dependent genes that were almost identical to those in the hnRNP K knockdown cells. Thus, we propose that hnRNP K affects Dbp-dependent genes through the poly(C) motif.

Overall, we propose that hnRNP K, which regulates *Dbp* mRNA oscillation, also affects other *Dbp*-dependent clock genes, such as *Per2*, *Rev-erbα*, and *RORβ* (Fig. 5B). Previously, we reported that knockdown of *Dbp* affected mRNA oscillation of other clock genes that contain D-box elements, such as *Per2*, *Rev-erbα*, and *RORβ* (41). This result indicates that high-amplitude *Dbp* oscillation is maintained through transcriptional activation by hnRNP K, which leads to the facilitation of the mRNA oscillation of other *Dbp*-dependent clock genes.

DISCUSSION

One of the main findings in this study is that high-amplitude *Dbp* mRNA oscillations are mediated by hnRNP K, which functions as a transcriptional activator. Prior to this study, it was reported that the poly(C) motif within the *Dbp* promoter could support high-amplitude *Dbp* mRNA oscillation (41). However, the *trans*-acting factors that could act on the poly(C) motif remained unclear. Here, we unveiled a *trans*-acting factor that maintains high-amplitude *Dbp* oscillation by interacting with the poly(C) motif. A recent study measured rhythmic H3K27ac enrichment and Pol2 density within the *Dbp* proximal promoter regions using ChIP-seq (47). Thus, we believe that rhythmic Pol2 recruitment could melt the promoter duplex DNA through the transcription initiation

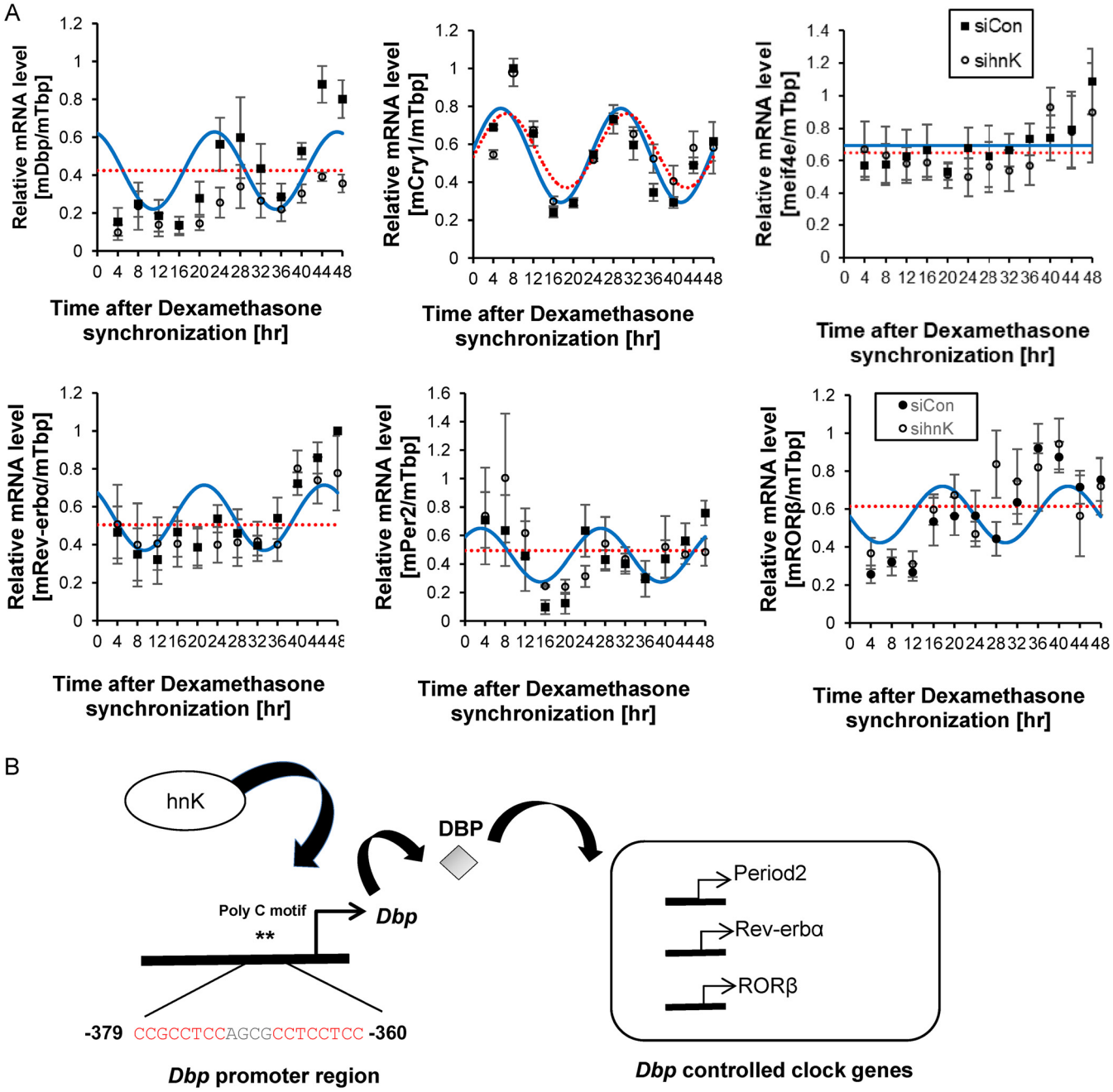

FIG 5 hnRNP K supports high-amplitude *Dbp* oscillation and *Dbp*-dependent clock genes such as *Period2*, *Rev-erbα*, and *RORβ*. (A) *Dbp*, *Cry1*, *eif4e*, *Rev-erbα*, *Per2*, and *RORβ* mRNA oscillations were measured after dexamethasone synchronization. CircWave, which is a program that is able to generate sine waves based on its algorithm, showed mRNA oscillation of each clock gene. The hnRNP K knockdown group showed a decrease in mRNA amplitude of *Dbp* and *Dbp*-dependent clock genes ($n = 3$ or 4; n.s., not significant). Error bars indicate SEM). sihnK, sihnRNP K. (B) Our proposed model of the regulation by hnRNP K, which leads to the regulation of *Dbp* and *Dbp*-dependent genes such as *Rev-erbα*, *Per2*, and *RORβ*. **, poly(C) motif.

complex, which could induce the interaction between TBP and hnRNP K (20, 24). Together with our study findings, this suggests that *Dbp* rhythmic transcription is regulated through a combined regulatory mechanism involving hnRNP K. We demonstrated that hnRNP K could indeed affect the circadian rhythm oscillation of *Dbp* mRNA by acting as a transcription activator along with other complex regulating mechanisms.

First, we screened several RNA-binding proteins by using RNA interference (RNAi) and identified hnRNP K, which may control the level of *Dbp* mRNA only (see Fig. S1 in the supplemental material). Next, we revealed that hnRNP K did not function as a *Dbp*

mRNA stabilizer (Fig. 1E). We also demonstrated that a specific promoter region of *Dbp* could be a target region of hnRNP K (Fig. 2). hnRNP K binds to single-stranded DNA to stabilize the secondary structure of DNA, thereby promoting transcription (24). Here, we determined hnRNP K to be the binding partner of the poly(C) motif within the *Dbp* promoter using an oligonucleotide pulldown assay (Fig. 3C and D). We also confirmed the binding of endogenous hnRNP K to the *Dbp* proximal promoter region, as well as its rhythmic interaction during circadian oscillation (Fig. 4A and B). This suggests that hnRNP K could function as a critical regulator of *Dbp* mRNA oscillation.

Furthermore, we measured the endogenous *Dbp* mRNA oscillation level after knockdown of hnRNP K (Fig. 5A). We demonstrated a decrease in the amplitude of *Dbp* mRNA oscillation by suppressing the level of hnRNP K. In addition to this, we verified mRNA oscillations of other *Dbp*-dependent clock genes that are affected by the knockdown of hnRNP K with or without the poly(C) motif within the Dbp promoter (Fig. 5A; see Fig. S9 in the supplemental material). We therefore suggest that circadian rhythm could be maintained by the level of hnRNP K. In summary, we demonstrated hnRNP K-mediated transcriptional regulation of *Dbp*, which is critical for the maintenance of high-amplitude *Dbp* and *Dbp*-dependent mRNA oscillations.

Here, we investigated the mechanistic relationship between hnRNP K and *Dbp* that results in delicate control of circadian rhythm in complicated biological systems. Although the precise mechanisms of rhythmic interaction and the involvement of hnRNP K in rhythmic cycling remain to be identified, we showed that hnRNP K-mediated transcription regulation impacts the oscillation of clock genes and proposed hnRNP K-dependent clocks.

MATERIALS AND METHODS

Cell culture and drug treatment. NIH 3T3 cells, poly(C)-deleted cells (41), and HEK293A cells were cultured in Dulbecco's modified Eagle's medium (HyClone) supplemented with 10% fetal bovine serum (HyClone) and 1% antibiotics (WelGENE) and were maintained in a humidified incubator with 95% air and 5% CO_2. NIH 3T3 cells were synchronized by treatment with 100 nM dexamethasone in 12-well plates containing $\sim 3.0 \times 10^5$ cells per well. After 2 h, the medium was replaced with complete medium, and the cells were harvested every 4 h for each sample (7). To measure mRNA decay kinetics, we blocked transcription by treating the NIH 3T3 cells with actinomycin D (5 μg/ml) and harvested them every 2 h for each sample.

Plasmids. We amplified several forms of mouse *Dbp* promoters (UCSC Genome Browser on Mouse, December 2011 [GRCm38/mm10] Assembly; https://genome.ucsc.edu), whose PCR products were inserted into the pGL3 basic vector, yielding pGL3 with the WT(Short) form of the *Dbp* promoter, the WT(Long) form of the *Dbp* promoter, serial deletion constructs (P1, P2, P3, P4, P5, and P6), and mutant constructs as previously reported (41).

Motif search and prediction. To perform comprehensive motif analysis, we used MEME-ChIP (http://meme-suite.org/tools/meme-chip). Here, we selected the classic mode for the motif discovery and enrichment. Next, we added the primary sequences of 1,056 promoter sequences described previously (29). We also added the motifs from "Eukaryote DNA" and "Vertebrates (*in vivo* and *in silico*)." For the width of the motifs, we allowed the minimum width of the motif to be "8" and the maximum width of the motif to be "10" and allowed MEME-ChIP to find 5 motifs (48). Gene Ontology for Motifs (GOMo) could extract the predicted functions, which provides the biological roles of the designated motifs (42, 43). The rank of "Top 5 specific predictions" was based upon the geometric mean score of rank sum tests for the particular gene ontology term.

RNA extraction and quantitative PCR. RNA extraction was performed as previously described (41). Endogenous mRNA levels were measured by using the StepOnePlus real-time PCR system (Applied Biosystems) with FastStart Universal SYBR green master mix (Roche). Specific primer pairs for mouse *Dbp* (NM_016974.3), mouse pre-*Dbp* (primers targeted an exon region and an intron region) (4), mouse *Per2* (NM_011066.3), mouse *Rev-erbα* (NM_145434.4), mouse *Hlf* (NM_172563.3), mouse *Tef* (NM_017376.3), mouse *Nfil3* (NM_017373.3) (11), mouse *Per3* (NM_001289877.1) (13), mouse hnRNP K (NM_001301341.1), and mouse *Eif4e* (NM_007917) were used for real-time PCR (the primer sequences are shown in Table S1 in the supplemental material).

Luciferase assay. By utilizing the Dual-Luciferase reporter assay system (Promega, USA), firefly and *Renilla* luciferase activities were quantified according to the manufacturer's instructions. Relative luciferase activities were determined as the ratio of firefly activity to *Renilla* activity.

Real-time luminescence. In 35-mm dishes, 5×10^5 NIH 3T3 fibroblasts (ATCC) were plated and transfected with 1 μg of WT(Short) and WT(Long) plasmids using Lipofectamine 2000 (Invitrogen) according to the manufacturer's instructions. Next, real-time luminescence was measured as previously described (41). Briefly, a Lumicycle device (Actimetrics) was maintained in a 37°C incubator for recording the samples, and luminescence was measured for 4 days. Lumicycle analysis software (Actimetrics) was used for data analysis.

ChIP assay. Treatment with glycine (0.125 M) for 10 min was used to stop the fixation reaction after 1% formaldehyde treatment in NIH 3T3 cells or poly(C)-deleted cells. The ChIP assay was performed as previously described (41). Anti-hnRNP K antibody (Abcam, ab70492) was added to immunoprecipitate hnRNP K. We also used protein G magnetic beads (Thermo Fisher, catalog number 88848) or protein A-agarose beads (Roche, catalog number 11719408001) to pull down hnRNP K. After that, we extracted DNA by using phenol-chloroform-isoamyl alcohol (25:24:1) (Affymetrix, catalog number 75831). Finally, DNA was resuspended in 1× TE buffer (10 mM Tris-Cl [pH 7.5], 1 mM EDTA) and used for quantification by quantitative PCR (the primer sequences are shown in Table S2 in the supplemental material).

Transient transfection and RNAi. Lipofectamine 2000 (Invitrogen), Metafectene (Bionex), and the Neon transfection system (Invitrogen) were used for transient transfection as recommended by the manufacturers. We transfected cells with 2 μg of luciferase reporter plasmid and maintained the cells in 6-well plates. For knockdown of RNA-binding proteins, including hnRNP K, we transfected cells with 2 μl of 20 μM siRNA and harvested them at 24 h after transfection. For hnRNP K knockdown or overexpression and subsequent luciferase assays, we transfected cells with 2 μl of 20 μM siRNA or 1 μg of hnRNP K-overexpressing vectors (HA-pcDNA vectors) 12 h prior to the transfection of cells with 1 μg luciferase reporter plasmid. We used specific siRNAs for hnRNP K siRNA pools (Bioneer) (13), hnRNP D (Dharmacon) (13), PTB (Bioneer) (13), hnRNP Q (Santa Cruz) (49), hnRNP R (Samchully Pharmaceuticals) (12), and hnRNP A1 (Bioneer) (11) to conduct knockdown of each target.

Oligonucleotide pulldown assay and mass spectrometry analysis. We used biotinylated oligonucleotides (Solgent, South Korea) for oligonucleotide pulldown assays. The biotinylated oligonucleotides had the following sequences: biotinylated wild type, 5′-CCG CCT CCA GCG CCT CCT CC-3′ (20-mer); and biotinylated mutant, 5′-AGG AAT ATA GCG ATT CAT AA-3′. After harvesting HEK293A cells, we lysed the cells using radioimmunoprecipitation assay (RIPA) buffer (10 mM Tris-Cl [pH 7.4], 1 mM EDTA, 0.1% SDS, 0.1% sodium deoxycholate, 1% Triton X-100) and centrifuged them at 15,000 rpm for 15 min at 4°C. The supernatant was used as the cell lysate for the binding assay. First, we washed streptavidin-agarose beads (Thermo Scientific, catalog number 20349) with RIPA buffer, and then we incubated the biotinylated oligonucleotide with either precleared cell lysate, GST, or GST-hnRNP K for 1 h. Next, we added the incubated material to freshly washed streptavidin-agarose beads and incubated them for 4 h at 4°C. The resin was then washed three times with RIPA buffer and boiled in sample buffer (40% glycerol, 240 mM Tris-HCl [pH 6.8], 8% SDS, 0.04% bromophenol blue, 5% beta-mercaptoethanol) at 95°C for 10 min. Finally, SDS-PAGE was conducted. After SDS-PAGE, the gel was stained with Coomassie brilliant blue R-250 (Sigma-Aldrich) for 30 min and destained with a solution of 30% methanol, 7% acetic acid, and 63% water. The gel was scanned for image acquisition, and the band of interest was sent to Genomine, Inc. (Pohang, South Korea) for mass spectrometry. In-gel proteolytic digestion and protein fragment extraction were conducted, and the results were compared with the NCBI protein database using Mascot software to identify the protein.

Protein extraction. GST and GST-hnRNP K were expressed in *Escherichia coli* BL21(DE3)/pLysS cells (Novagen) grown to an absorbance at 600 nm (A_{600}) of 0.6. Induction of GST and GST-hnRNP K was performed with 0.5 mM isopropyl-β-D-1-thiogalactopyranoside (IPTG) overnight at 18°C. Next, cells were resuspended in 20 mM Tris-HCl (pH 7.5), 150 mM NaCl, 1% Triton-X, 1 mM dithiothreitol, and protease inhibitor cocktail (Roche) and were lysed by sonication. GST and GST-hnRNP K were purified using glutathione-Sepharose 4B-agarose beads (GE Healthcare Bio-Sciences) and were eluted in 50 mM Tris-HCl (pH 8.0) and 20 mM reduced L-glutathione (GE Healthcare).

Immunoblot assay. Immunoblotting was conducted by using polyclonal anti-hnRNP K (Abcam, ab70492), monoclonal anti-GST (Santa Cruz, sc-138), monoclonal anti-HA (Abcam, 12CA5), and monoclonal anti-GAPDH (Santa Cruz, sc-47724) as primary antibodies. A Supex ECL solution kit (Neuronex) and LAS-4000 chemiluminescence detection system (Fujifilm) were used after horseradish peroxidase-conjugated species-specific secondary antibody (goat, Santa Cruz Biotechnology; guinea pig, Santa Cruz Biotechnology; mouse, Thermo Scientific; rabbit, Jackson ImmunoResearch Laboratories) reactions, and Image Gauge (Fuji Film) was used for the analysis of the acquired images according to the manufacturer's instructions.

MTT assay. NIH 3T3 cells at a density of 2×10^4 cells per well in 96-well plates were transfected with control (siCon) and hnRNP K (sihnRNP K) siRNAs. After 48 h, MTT (5 mg/ml) was added to each well, followed by a 2-h incubation at room temperature. Next, the medium was removed, and 100 μl dimethyl sulfoxide (DMSO) was added to each well. Color development was allowed to proceed for 3 h at room temperature in the dark. Finally, we measured the absorbance of each well at 570 nm using a NanoQuant spectrophotometer (Tecan).

Statistical analysis. Graphs are plotted as a mean ± standard error of the mean (SEM). Two-way ANOVA was used to conduct grouped analyses with multiple groups by Sidak's multiple-comparison test. One-way ANOVA was used to conduct column analyses with more than two groups with Tukey's multiple-comparison test, analyzed with Prism software. CircWave software was also used to confirm mRNA oscillation, which generates sine waves based on its algorithm.

Data availability. Data for hnRNP K bound genes are available in reference 29. MEME-ChIP and GOMo (Gene Ontology for Motifs) algorithms are available at http://meme-suite.org/.

SUPPLEMENTAL MATERIAL

Supplemental material is available online only.

SUPPLEMENTAL FILE 1, PDF file, 1.2 MB.

ACKNOWLEDGMENTS

We thank Ze'ev Ronai (Sanford Burnham Prebys Medical Discovery Institute) for providing HA-hnRNP K WT and Sung-Hoon Kim (McGill University) for providing the GST-hnRNP K plasmid.

This work was supported by the Bio & Medical Technology Development Program of the National Research Foundation (NRF) funded by the Korean government (MSIT) (no. 2017M3C7A1023478), by the National Research Foundation of Korea (NRF) funded by the Korean government (MEST) (no. 2019R1A2C2009440), by the Cooperative Research Program for Agriculture Science & Technology Development (project no. PJ01324801) of the Rural Development Administration, and by BK21 Plus funded by the Ministry of Education, Republic of Korea (10Z20130012243).

We declare no conflict of interest.

REFERENCES

1. Yu W, Hardin PE. 2006. Circadian oscillators of Drosophila and mammals. J Cell Sci 119:4793–4795. https://doi.org/10.1242/jcs.03174.
2. Lowrey PL, Takahashi JS. 2004. Mammalian circadian biology: elucidating genome-wide levels of temporal organization. Annu Rev Genomics Hum Genet 5:407–441. https://doi.org/10.1146/annurev.genom.5.061903.175925.
3. Koike N, Yoo SH, Huang HC, Kumar V, Lee C, Kim TK, Takahashi JS. 2012. Transcriptional architecture and chromatin landscape of the core circadian clock in mammals. Science 338:349–354. https://doi.org/10.1126/science.1226339.
4. Stratmann M, Suter DM, Molina N, Naef F, Schibler U. 2012. Circadian Dbp transcription relies on highly dynamic BMAL1-CLOCK interaction with E boxes and requires the proteasome. Mol Cell 48:277–287. https://doi.org/10.1016/j.molcel.2012.08.012.
5. Kim TD, Woo KC, Cho S, Ha DC, Jang SK, Kim KT. 2007. Rhythmic control of AANAT translation by hnRNP Q in circadian melatonin production. Genes Dev 21:797–810. https://doi.org/10.1101/gad.1519507.
6. Lim I, Jung Y, Kim DY, Kim KT. 2016. HnRNP Q has a suppressive role in the translation of mouse cryptochrome1. PLoS One 11:e0159018. https://doi.org/10.1371/journal.pone.0159018.
7. Lee KH, Woo KC, Kim DY, Kim TD, Shin J, Park SM, Jang SK, Kim KT. 2012. Rhythmic interaction between Period1 mRNA and hnRNP Q leads to circadian time-dependent translation. Mol Cell Biol 32:717–728. https://doi.org/10.1128/MCB.06177-11.
8. Jung Y, Ryu HG, Kim SW, Lee KH, Gu S, Yi H, Ku HO, Jang SK, Kim KT. 2019. The RNA-binding protein hnRNP Q represses translation of the clock gene Bmal1 in murine cells. J Biol Chem 294:7682–7691. https://doi.org/10.1074/jbc.RA118.006947.
9. Kim DY, Woo KC, Lee KH, Kim TD, Kim KT. 2010. hnRNP Q and PTB modulate the circadian oscillation of mouse Rev-erb alpha via IRES-mediated translation. Nucleic Acids Res 38:7068–7078. https://doi.org/10.1093/nar/gkq569.
10. Woo KC, Ha DC, Lee KH, Kim DY, Kim TD, Kim KT. 2010. Circadian amplitude of cryptochrome 1 is modulated by mRNA stability regulation via cytoplasmic hnRNP D oscillation. Mol Cell Biol 30:197–205. https://doi.org/10.1128/MCB.01154-09.
11. Kim HJ, Lee HR, Seo JY, Ryu HG, Lee KH, Kim DY, Kim KT. 2017. Heterogeneous nuclear ribonucleoprotein A1 regulates rhythmic synthesis of mouse Nfil3 protein via IRES-mediated translation. Sci Rep 7:42882. https://doi.org/10.1038/srep42882.
12. Lee HR, Kim TD, Kim HJ, Jung Y, Lee D, Lee KH, Kim DY, Woo KC, Kim KT. 2015. Heterogeneous ribonucleoprotein R regulates arylalkylamine N-acetyltransferase synthesis via internal ribosomal entry site-mediated translation in a circadian manner. J Pineal Res 59:518–529. https://doi.org/10.1111/jpi.12284.
13. Kim SH, Lee KH, Kim DY, Kwak E, Kim S, Kim KT. 2015. Rhythmic control of mRNA stability modulates circadian amplitude of mouse Period3 mRNA. J Neurochem 132:642–656. https://doi.org/10.1111/jnc.13027.
14. Matunis MJ, Michael WM, Dreyfuss G. 1992. Characterization and primary structure of the poly(C)-binding heterogeneous nuclear ribonucleoprotein complex K protein. Mol Cell Biol 12:164–171. https://doi.org/10.1128/mcb.12.1.164.
15. Hovemann BT, Reim I, Werner S, Katz S, Saumweber H. 2000. The protein Hrb57A of Drosophila melanogaster closely related to hnRNP K from vertebrates is present at sites active in transcription and coprecipitates with four RNA-binding proteins. Gene 245:127–137. https://doi.org/10.1016/s0378-1119(00)00027-5.
16. Charroux B, Angelats C, Fasano L, Kerridge S, Vola C. 1999. The levels of the bancal product, a Drosophila homologue of vertebrate hnRNP K protein, affect cell proliferation and apoptosis in imaginal disc cells. Mol Cell Biol 19:7846–7856. https://doi.org/10.1128/mcb.19.11.7846.
17. Bomsztyk K, Denisenko O, Ostrowski J. 2004. hnRNP K: one protein multiple processes. Bioessays 26:629–638. https://doi.org/10.1002/bies.20048.
18. Preußner M, Goldammer G, Neumann A, Haltenhof T, Rautenstrauch P, Müller-McNicoll M, Heyd F. 2017. Body temperature cycles control rhythmic alternative splicing in mammals. Mol Cell 67:433–446. https://doi.org/10.1016/j.molcel.2017.06.006.
19. McGlincy NJ, Valomon A, Chesham JE, Maywood ES, Hastings MH, Ule J. 2012. Regulation of alternative splicing by the circadian clock and food related cues. Genome Biol 13:R54. https://doi.org/10.1186/gb-2012-13-6-r54.
20. Michelotti EF, Michelotti GA, Aronsohn AI, Levens D. 1996. Heterogeneous nuclear ribonucleoprotein K is a transcription factor. Mol Cell Biol 16:2350–2360. https://doi.org/10.1128/mcb.16.5.2350.
21. Shnyreva M, Schullery DS, Suzuki H, Higaki Y, Bomsztyk K. 2000. Interaction of two multifunctional proteins. Heterogeneous nuclear ribonucleoprotein K and Y-box-binding protein. J Biol Chem 275:15498–15503. https://doi.org/10.1074/jbc.275.20.15498.
22. Tomonaga T, Levens D. 1996. Activating transcription from single stranded DNA. Proc Natl Acad Sci U S A 93:5830–5835. https://doi.org/10.1073/pnas.93.12.5830.
23. Michelotti GA, Michelotti EF, Pullner A, Duncan RC, Eick D, Levens D. 1996. Multiple single-stranded cis elements are associated with activated chromatin of the human c-myc gene in vivo. Mol Cell Biol 16:2656–2669. https://doi.org/10.1128/mcb.16.6.2656.
24. Banerjee K, Wang M, Cai E, Fujiwara N, Baker H, Cave JW. 2014. Regulation of tyrosine hydroxylase transcription by hnRNP K and DNA secondary structure. Nat Commun 5:5769. https://doi.org/10.1038/ncomms6769.
25. Ritchie SA, Pasha MK, Batten DJ, Sharma RK, Olson DJ, Ross AR, Bonham K. 2003. Identification of the SRC pyrimidine-binding protein (SPy) as hnRNP K: implications in the regulation of SRC1A transcription. Nucleic Acids Res 31:1502–1513. https://doi.org/10.1093/nar/gkg246.
26. Takimoto M, Tomonaga T, Matunis M, Avigan M, Krutzsch H, Dreyfuss G, Levens D. 1993. Specific binding of heterogeneous ribonucleoprotein particle protein K to the human c-myc promoter, in vitro. J Biol Chem 268:18249–18258.
27. Uribe DJ, Guo K, Shin YJ, Sun D. 2011. Heterogeneous nuclear ribonucleoprotein K and nucleolin as transcriptional activators of the vascular endothelial growth factor promoter through interaction with secondary DNA structures. Biochemistry 50:3796–3806. https://doi.org/10.1021/bi101633b.
28. Lynch M, Chen L, Ravitz MJ, Mehtani S, Korenblat K, Pazin MJ, Schmidt EV. 2005. hnRNP K binds a core polypyrimidine element in the eukaryotic translation initiation factor 4E (eIF4E) promoter, and its regulation of eIF4E contributes to neoplastic transformation. Mol Cell Biol 25:6436–6453. https://doi.org/10.1128/MCB.25.15.6436-6453.2005.
29. Huarte M, Guttman M, Feldser D, Garber M, Koziol MJ, Kenzelmann-Broz

D, Khalil AM, Zuk O, Amit I, Rabani M, Attardi LD, Regev A, Lander ES, Jacks T, Rinn JL. 2010. A large intergenic noncoding RNA induced by p53 mediates global gene repression in the p53 response. Cell 142:409–419. https://doi.org/10.1016/j.cell.2010.06.040.
30. Wuarin J, Schibler U. 1990. Expression of the liver-enriched transcriptional activator protein DBP follows a stringent circadian rhythm. Cell 63:1257–1266. https://doi.org/10.1016/0092-8674(90)90421-A.
31. Mueller CR, Maire P, Schibler U. 1990. DBP, a liver-enriched transcriptional activator, is expressed late in ontogeny and its tissue specificity is determined posttranscriptionally. Cell 61:279–291. https://doi.org/10.1016/0092-8674(90)90808-r.
32. Yang S, Van Dongen HPA, Wang K, Berrettini W, Bućan M. 2009. Assessment of circadian function in fibroblasts of patients with bipolar disorder. Mol Psychiatry 14:143–155. https://doi.org/10.1038/mp.2008.10.
33. Mitsui S, Yamaguchi S, Matsuo T, Ishida Y, Okamura H. 2001. Antagonistic role of E4BP4 and PAR proteins in the circadian oscillatory mechanism. Genes Dev 15:995–1006. https://doi.org/10.1101/gad.873501.
34. Wuarin J, Falvey E, Lavery D, Talbot D, Schmidt E, Ossipow V, Fonjallaz P, Schibler U. 1992. The role of the transcriptional activator protein DBP in circadian liver gene expression. J Cell Sci Suppl 16:123–127. https://doi.org/10.1242/jcs.1992.supplement_16.15.
35. Ueda HR, Hayashi S, Chen W, Sano M, Machida M, Shigeyoshi Y, Iino M, Hashimoto S. 2005. System-level identification of transcriptional circuits underlying mammalian circadian clocks. Nat Genet 37:187–192. https://doi.org/10.1038/ng1504.
36. Falvey E, Marcacci L, Schibler U. 1996. DNA-binding specificity of PAR and C/EBP leucine zipper proteins: a single amino acid substitution in the C/EBP DNA-binding domain confers PAR-like specificity to C/EBP. Biol Chem 377:797–809.
37. Takahashi JS. 2017. Transcriptional architecture of the mammalian circadian clock. Nat Rev Genet 18:164–179. https://doi.org/10.1038/nrg.2016.150.
38. Ripperger JA, Shearman LP, Reppert SM, Schibler U. 2000. CLOCK, an essential pacemaker component, controls expression of the circadian transcription factor DBP. Genes Dev 14:679–689.
39. Ripperger JA, Schibler U. 2006. Rhythmic CLOCK-BMAL1 binding to multiple E-box motifs drives circadian Dbp transcription and chromatin transitions. Nat Genet 38:369–374. https://doi.org/10.1038/ng1738.
40. Stratmann M, Stadler F, Tamanini F, van der Horst GT, Ripperger JA. 2010. Flexible phase adjustment of circadian albumin D site-binding protein (DBP) gene expression by CRYPTOCHROME1. Genes Dev 24:1317–1328. https://doi.org/10.1101/gad.578810.
41. Kwon PK, Kim H-M, Kim SW, Kang B, Yi H, Ku H-O, Roh T-Y, Kim K-T. 2019. The poly(C) motif in the proximal promoter region of D site-binding protein gene (*Dbp*) drives its high-amplitude oscillation. Mol Cell Biol 39:e00101-19. https://doi.org/10.1128/MCB.00101-19.
42. Boden M, Bailey TL. 2008. Associating transcription factor-binding site motifs with target GO terms and target genes. Nucleic Acids Res 36:4108–4117. https://doi.org/10.1093/nar/gkn374.
43. Buske FA, Boden M, Bauer DC, Bailey TL. 2010. Assigning roles to DNA regulatory motifs using comparative genomics. Bioinformatics 26:860–866. https://doi.org/10.1093/bioinformatics/btq049.
44. Braddock DT, Baber JL, Levens D, Clore GM. 2002. Molecular basis of sequence-specific single-stranded DNA recognition by KH domains: solution structure of a complex between hnRNP K KH3 and single-stranded DNA. EMBO J 21:3476–3485. https://doi.org/10.1093/emboj/cdf352.
45. Choi HS, Hwang CK, Song KY, Law PY, Wei LN, Loh HH. 2009. Poly(C)-binding proteins as transcriptional regulators of gene expression. Biochem Biophys Res Commun 380:431–436. https://doi.org/10.1016/j.bbrc.2009.01.136.
46. Dickey TH, Altschuler SE, Wuttke DS. 2013. Single-stranded DNA-binding proteins: multiple domains for multiple functions. Structure 21:1074–1084. https://doi.org/10.1016/j.str.2013.05.013.
47. Sobel JA, Krier I, Andersin T, Raghav S, Canella D, Gilardi F, Kalantzi AS, Rey G, Weger B, Gachon F, Dal Peraro M, Hernandez N, Schibler U, Deplancke B, Naef F, CycliX Consortium. 2017. Transcriptional regulatory logic of the diurnal cycle in the mouse liver. PLoS Biol 15:e2001069. https://doi.org/10.1371/journal.pbio.2001069.
48. Machanick P, Bailey TL. 2011. MEME-ChIP: motif analysis of large DNA datasets. Bioinformatics 27:1696–1697. https://doi.org/10.1093/bioinformatics/btr189.
49. Choi JH, Kim SH, Jeong YH, Kim SW, Min KT, Kim KT. 2019. hnRNP Q regulates internal ribosome entry site-mediated *fmr1* translation in neurons. Mol Cell Biol 39:e00371-18. https://doi.org/10.1128/MCB.00371-18.